CrossMark

A three-step Oseen correction method for the steady Navier–Stokes equations

Yueqiang Shang

Abstract We present and analyze a two-grid scheme based on mixed finite element approximations for the steady incompressible Navier–Stokes equations. This numerical scheme aims at the simulations of high Reynolds number flows and consists of three steps: in the first step, we solve a finite element variational multiscale-stabilized nonlinear Navier–Stokes system on a coarse mesh, and then, in the second and third steps, we solve Oseen-linearized and -stabilized problems which have the same stiffness matrices with only different right-hand sides on a fine mesh. We provide error bounds for the approximate solutions, derive algorithmic parameter scalings from the analysis, and present some numerical results to verify the theoretical predictions and demonstrate the effectiveness of the proposed method.

1 Introduction

We consider the incompressible Navier–Stokes equations on a bounded domain $\Omega \subset \mathbb{R}^d$ (d=2 or 3):

$$-\nu \Delta u + (u \cdot \nabla)u + \nabla p = f \quad \text{in } \Omega, \tag{1}$$

$$\nabla \cdot u = 0 \quad \text{in } \Omega, \tag{2}$$

subject to homogeneous Dirichlet boundary conditions $u = 0$ on $\partial\Omega$. In the above equations, $u = (u_1(x), \ldots, u_d(x))^T$ denotes the velocity field, $p = p(x)$ denotes the pressure, $f = (f_1(x), \ldots, f_d(x))^T$ a given body force field, and $\nu > 0$ is the viscosity of fluid. Let U be a characteristic velocity and L a characteristic length, then the Reynolds number is defined as $Re = UL/\nu$.

Y. Shang (✉)
School of Mathematics and Statistics, Southwest University, Chongqing 400715, People's Republic of China
e-mail: yqshang@swu.edu.cn

In this paper, we are interested in the simulation of the above Navier–Stokes equations at high Reynolds numbers or with small viscosities. It is well understood that when the Reynolds number increases, the Navier–Stokes equations become convection dominated, causing troubles for the classical Galerkin finite element methods which may lead to spurious oscillations. Therefore, stabilization methods are essential in simulation of the Navier–Stokes equations at high Reynolds numbers. Among various stabilization methods in the literature, we are here interested in a finite element variational multiscale method based on two local Gauss integrations presented by Zheng et al. in [1]. The idea of two local Gauss integrations was first considered in [2,3] to stabilize the equal-order $P_1 - P_1$ elements approximations of Stokes and Navier–Stokes equations, which can be viewed as an variant of the general stabilization method of Bochev and co-workers [4]. As we will see later, this finite element variational multiscale method based on two local Gauss integrations is equivalent to a LPS (local projection stabilization, cf. [5,6])-like method for these mixed finite element approximations where the interpolation of velocity is of second order. Its advantage over the commonly used projection-based variational multiscale methods (see, e.g., [7] and references therein) is that it is easy to implement, free of extra storage, and hence has attracted considerable attentions from researchers (cf. [8–14]).

In this paper, by combining the above-mentioned finite element variational multiscale method based on two local Gauss integrations with two-grid discretization strategy, we present a three-step Oseen correction method for the Navier–Stokes equations at high Reynolds numbers. The method proceeds as follows:

– Step 1: Begin by solving a finite element variational multiscale-stabilized nonlinear Navier–Stokes system for (u_H, p_H) upon a coarse mesh of width H.
– Step 2: Pass the coarse mesh solution u_H to the fine mesh of width h and solve a discrete finite element variational multiscale-stabilized Oseen problem for (u_h^*, p_h^*).
– Step 3: Solve a discrete Oseen problem (which has the same stiffness matrix as Step 2, with only different right-hand side involving u_H and u_h^*) for the update (u^h, p^h) upon the same fine mesh.

Our theoretical analysis shows that, if we choose $h \sim H^{(s+1)/s}$ for a certain integer s, the approximate solution (u^h, p^h) produced by the three-step Oseen correction method is asymptotically as accurate as the approximation produced by solving directly the finite element variational multiscale-stabilized Navier–Stokes system on the fine mesh. We numerically demonstrate that each step of the method significantly improves the accuracy of the approximate solution of the previous step. The novelty of the presented three-step Oseen correction method is that it combines the best algorithmic features of the two-grid discretization strategy and the finite element variational multiscale method, as well as the Oseen linearization. Specifically, on the one hand, it allows high Reynolds number flows that are challenging to simulate for the standard two-grid methods. On the other hand, it can save a large amount of computational time compared with the one-level finite element variational multiscale method used directly on the fine mesh. An additional decoration to the proposed method consists in using an Oseen-type partial linearization for the fine mesh corrections, making the resulting linear systems be more tractable than the ones from the commonly used full linearizations based on Newton iterations, such as those in [15–17]. Moreover, with the extra third step, the presented method can yield a much better approximate solution with a greater accuracy compared with the standard stabilized two-grid method based on Oseen correction.

Two-grid discretization strategy is a well-established technique for steady nonlinear elliptic PDEs, see [18–20]. The basic idea is to capture the low modes or global solution envelope by solving an initial nonlinear approximation problem on a coarse mesh, and then capture the fine structures by computing a linearized system on a fine mesh. This two-grid discretization strategy has been applied to numerically solving the steady Navier–Stokes equations by Layton [15], Dai and Cheng [21], He et al. [22–25], Liu and Hou [26]. It was also combined with the subgrid stabilization method [17,27,28] and the domain decomposition method [29–31]. Two-grid methods for the unsteady Navier–Stokes equations were also studied in [32–39]. In most of the above works, a full linearization of the nonlinear Navier–Stokes system based on Newton's method is used to define the fine mesh problem, and consequently, the resulting linear systems of equations are generally both highly nonsymmetric and indefinite. As mentioned before, by means of an Oseen-type partial linearization studied herein, the linear systems originating from the fine mesh problem become more tractable. The Oseen-type linearization had also been used extensively in, e.g., [40–44] to resolve the nonlinearity in the Navier–Stokes system. It is worth mentioning that there are other types of two-grid

methods (see, e.g., [45–48]) which are preconditioning methods for a given discretization scheme, not for designing a discretization scheme as studied herein.

The rest of the paper proceeds as follows. In Sect. 2, we introduce some notations and preliminaries. In Sect. 3, we present and analyze the three-step Oseen correction method. Section 4 shows some numerical results followed by conclusions in Sect. 5.

2 Preliminaries and notations

2.1 Functional setting of the Navier–Stokes equations

In this paper, for an integer $k \geq 1$, $H^k(\Omega)^d$ denotes the usual Sobolev spaces of functions with kth distributional derivatives in $L^2(\Omega)^d$ and equipped with norms $\| \cdot \|_k$. $H_0^1(\Omega)^d$ is the subspace of $H^1(\Omega)^d$ of functions trace of which is zero on $\partial \Omega$ and $L_0^2(\Omega)$ is the space of $L^2(\Omega)$ functions mean value of which is zero. $(\cdot, \cdot)$ denotes the the standard inner-product of $L^2(\Omega)$ or $L^2(\Omega)^d$ (cf. [49]). We will denote by $\| \cdot \|_{-1}$ the norm of the dual space of $H_0^1(\Omega)^d$. The letter c or C (with or without subscript) stands for a generic positive constant which is independent of the viscosity ν, the stabilization, and mesh parameters, and may stand for different values at its different occurrences.

Let

$$X = H_0^1(\Omega)^d, \quad Y = L^2(\Omega)^d, \quad M = L_0^2(\Omega).$$

We define

$$b(u, v, w) = ((u \cdot \nabla)v, w) + \frac{1}{2}((\nabla \cdot u)v, w)$$
$$= \frac{1}{2}((u \cdot \nabla)v, w) - \frac{1}{2}((u \cdot \nabla)w, v), \quad \forall u, v, w \in X,$$

which has the following properties (cf. [50–54]):

$$b(u, v, w) = -b(u, w, v), \quad \forall u, v, w \in X, \tag{3}$$

$$|b(u, v, w)| \leq N \|\nabla u\|_0 \|\nabla v\|_0 \|\nabla w\|_0, \quad \forall u, v, w \in X, \tag{4}$$

$$|b(u, v, w)| \leq c \|u\|_0 \|\nabla v\|_0 \|w\|_2, \quad \forall u, v \in X, w \in H^2(\Omega)^d, \tag{5}$$

where N and c are positive constants depending only on Ω. The weak form of (1)–(2) reads: find a pair $(u, p) \in X \times M$ such that

$$\nu(\nabla u, \nabla v) + b(u, u, v) - (\nabla \cdot v, p) + (\nabla \cdot u, q) = (f, v), \quad \forall (v, q) \in X \times M. \tag{6}$$

A nonsingular solution u of the Navier–Stokes equations is defined as [55]

$$\inf_{v \in V} \sup_{w \in V} \frac{\nu(\nabla v, \nabla w) + b(u, v, w) + b(v, u, w)}{\|\nabla v\|_0 \|\nabla w\|_0} \geq \sigma > 0, \tag{7}$$

and satisfies (cf. [56])

$$\|\nabla u\|_0 \leq \nu^{-1} \|f\|_{-1}, \quad \|f\|_{-1} = \sup_{v \in X, v \neq 0} \frac{|(f, v)|}{\|\nabla v\|_0}, \tag{8}$$

where $\sigma = \sigma(\nu, u)$ (see [51]) is a constant and $V = \{v \in X : (\nabla \cdot v, q) = 0, \ \forall q \in M\}$.

2.2 Mixed finite element spaces

Let $\mu > 0$ be a discretization parameter. For each μ, let $T^\mu(\Omega) = \{K\}$ be a regular family of triangulations of $\overline{\Omega}$ (see, e.g., [51]), consisting of triangles (when $d = 2$) or tetrahedrons (when $d = 3$). For each triangle or tetrahedron K, we denote by μ_K the diameter of K and by μ the maximum of μ_K. Let (X_μ, M_μ) be a pair of compatible finite element spaces for discretizing the velocity and the pressure. We assume that the following Ladyzhenskaya–Babuska–Brezzi (LBB) condition holds:

$$\beta \|q\|_0 \leq \sup_{v \in X_\mu, v \neq 0} \frac{(\nabla \cdot v, q)}{\|\nabla v\|_0}, \quad \forall q \in M_\mu, \tag{9}$$

and for each $(u, p) \in H^{k+1}(\Omega)^d \times H^k(\Omega)$ $(1 \leq k)$, there is an approximation pair $(\pi_\mu u, \rho_\mu p) \in X_\mu \times M_\mu$ such that

$$\|u - \pi_\mu u\|_1 \leq c\mu^s \|u\|_{1+s}, \quad \|p - \rho_\mu p\|_0 \leq c\mu^s \|p\|_s, \quad 1 \leq s \leq k, \tag{10}$$

where $\beta > 0$ is a constant.

We consider those LBB stable, mixed finite element approximations where the finite element interpolant for the velocity is of second order. Examples of such compatible, mixed finite element pairs are the Taylor–Hood $(P_2 - P_1)$ elements [57], the $P_2 - P_0$ elements [58], the augmented $P_2 - P_1$ elements [59,60], and the Scott–Vogelius $(P_2 - P_1^{\text{disc}})$ elements under the restriction that the mesh is a barycenter refinement of a regular mesh when $d = 2$ or a Powell–Sabin tetrahedralization when $d = 3$ (see [61–63] for details).

We define

$$V_\mu = \{v_\mu \in X_\mu : (\nabla \cdot v_\mu, q_\mu) = 0, \ \forall q_\mu \in M_\mu\},$$

and have [51,56]

$$\inf_{v_\mu \in V_\mu} \|\nabla(v - v_\mu)\|_0 \leq c \left(1 + \frac{1}{\beta}\right) \inf_{v_\mu \in X_\mu} \|\nabla(v - v_\mu)\|_0, \quad \forall v \in V. \tag{11}$$

2.3 The stabilization term

We define the stabilization term as follows [1]:

$$G_\mu(u_\mu, v_\mu) = \alpha_\mu \sum_{K \in T^\mu(\Omega)} \left(\int_{K,m} \nabla u_\mu \cdot \nabla v_\mu \mathrm{d}x - \int_{K,1} \nabla u_\mu \cdot \nabla v_\mu \mathrm{d}x \right), \quad \forall u_\mu, v_h \in X_\mu, \tag{12}$$

where $\int_{K,m}(\cdot)\mathrm{d}x$ $(m \geq 2)$ denotes the mth-order Gauss integral over the element K and $\int_{K,1}(\cdot)\mathrm{d}x$ the first-order Gauss integral over the element K. $\alpha_\mu > 0$ is the stabilization coefficient.

Let P_0 be the piecewise constant space on the element K, so that we set

$$R_0 = \left\{ v \in L^2(\Omega) : v|_K \in P_0, \quad \forall K \in T^\mu(\Omega) \right\}, \quad L_\mu = R_0^{d \times d}, \quad L = L^2(\Omega)^{d \times d},$$

and define L^2-orthogonal projection $\Pi_\mu : L \to L_\mu$, which projects onto the piecewise constant space, can be computed locally and satisfies

$$(\Pi_\mu \nabla u, v) = (\nabla u, v), \quad \forall u \in X, v \in L_\mu, \tag{13}$$

$$\|\Pi_\mu \nabla v\|_0 \leq \|\nabla v\|_0, \quad \forall v \in X, \tag{14}$$

$$\|(I - \Pi_\mu)\nabla v\|_0 \leq \|\nabla v\|_0, \quad \forall v \in X. \tag{15}$$

Then the stabilization term (12) can be rewritten as [1]

$$G_\mu(u_\mu, v_\mu) = \alpha_\mu((I - \Pi_\mu)\nabla u_h, (I - \Pi_\mu)\nabla v_\mu) = \alpha_\mu(\nabla u_\mu, \nabla v_\mu) - \alpha_\mu(\Pi_\mu \nabla u_\mu, \nabla v_\mu). \tag{16}$$

Remark 2.1 The equivalence of the stabilizations (12) and (16) is only valid for those mixed finite element pairs where the interpolant of the velocity is of second order (see [1] for details). However, our following error estimates based on the stabilization (16) are also valid for higher-order LBB stable elements $P_k - P_{k-1}(k \geq 2)$ and non-LBB stable elements such as equal-order $P_k - P_k(k \geq 2)$ elements (in such a case, appropriate pressure stabilizations should be added to the formulation).

3 Three-step Oseen correction method

In our method, we need two levels meshes: a coarse mesh $T^H(\Omega)$ of width H and a fine mesh $T^h(\Omega)$ of width h $(0 < h < H < 1)$. We assume they are nested since it will simplify our analysis substantially. Let (X_H, M_H) be a pair of compatible finite element spaces associated with the coarse mesh $T^H(\Omega)$, and (X_h, M_h) the one associated with the fine mesh $T^h(\Omega)$. Then our three-step Oseen correction method is stated as follows.

Algorithm I: Three-step Oseen correction algorithm.
   Step 1: Find a coarse mesh solution $(u_H, p_H) \in X_H \times M_H$ satisfying

$$\nu(\nabla u_H, \nabla v_H) + b(u_H, u_H, v_H) - (\nabla \cdot v_H, p_H) + (\nabla \cdot u_H, q_H) + G_H(u_H, v_H) = (f, v_H),$$
$$\forall (v_H, q_H) \in X_H \times M_H. \tag{17}$$

   Step 2: Find a fine mesh solution $(u_h^*, p_h^*) \in X_h \times M_h$ such that for all $(v_h, q_h) \in X_h \times M_h$

$$\nu(\nabla u_h^*, \nabla v_h) + b(u_H, u_h^*, v_h) - (\nabla \cdot v_h, p_h^*) + (\nabla \cdot u_h^*, q) + G_h(u_h^*, v_h) = (f, v_h) \tag{18}$$

   Step 3: Find $(u^h, p^h) \in X_h \times M_h$ such that

$$\nu(\nabla u^h, \nabla v_h) + b(u_H, u^h, v_h) - (\nabla \cdot v_h, p^h) + (\nabla \cdot u^h, q_h) + G_h(u^h, v_h)$$
$$= (f, v_h) + b(u_H - u_h^*, u_h^*, v_h), \quad \forall (v_h, q_h) \in X_h \times M_h. \tag{19}$$

Remark 3.1 It is worth mentioning that on the left side of (19) in the above algorithm, we linearize the nonlinear convection term by $b(u_H, u^h, v_h)$ rather than $b(u_h^*, u^h, v_h)$ as used usually in the standard Newton or Oseen iterations. There are two reasons for this. First, by using u_H instead of the newly computed solution u_h^* to linearize the nonlinearity, we keep the same coefficient matrices as the previous step. Second, since there is a term $b(u_H - u_h^*, u_h^*, v_h)$ in the right-hand side of (19), Step 3 differs from the standard Newton or Oseen iterations which usually use the solution newly computed at the previous iteration step to linearize the nonlinearity in the current iteration step. In fact, our numerical results show that replacing $b(u_H, u^h, v_h)$ by $b(u_h^*, u^h, v_h)$ in the left-hand side of (19) will degrade the accuracy of the approximate solutions.

We now give basic error analysis for Algorithm I in the natural energy norm for the Navier–Stokes equations. At the beginning, we introduce some notations and definitions:

$$\kappa_1 = \nu + \alpha_H + 2\nu^{-1}N\|f\|_{-1}, \quad \kappa_2 = \nu + \alpha_h + \nu^{-1}N\|f\|_{-1},$$
$$\delta = \nu^{-1}(\nu + \alpha_h)^{-1}\|f\|_{-1}.$$

By a standard argument (cf. [13]), we have the following results for the approximate solution of Step 1:

Theorem 3.1 *Assume $(u, p) \in (X \cap H^{k+1}(\Omega)^d) \times (M \cap H^k(\Omega))$ be the exact solution of the Navier–Stokes equations, and α_H tends to zero as H tends to zero. Then, there is $H_0 > 0$ such that for all $H \in (0, H_0]$, the approximate solution (u_H, p_H) of Step 1 in Algorithm I satisfies*

$$\|\nabla u_H\|_0 \leq \nu^{-1}\|f\|_{-1}, \tag{20}$$

$$\|\nabla(u - u_H)\|_0 \leq C(\beta)\left(1 + \frac{2\kappa_1}{\sigma}\right)\inf_{w_H \in X_H}\|\nabla(u - w_H)\|_0 + \frac{2}{\sigma}\inf_{\lambda_H \in M_H}\|p - \lambda_h\|_0 + \frac{4\alpha_H}{\nu\sigma}\|f\|_{-1}, \tag{21}$$

$$\|p - p_H\|_0 \leq \left(1 + \frac{1}{\beta}\right)\inf_{\lambda_h \in M_H}\|p - \lambda_h\|_0 + \frac{\kappa_1}{\beta}\|\nabla(u - u_H)\|_0 + \frac{2\alpha_H}{\nu\beta}\|f\|_{-1}. \tag{22}$$

$$\|u - u_H\|_0 + \|p - p_H\|_{-1} \leq c_1 H\left(\|\nabla(u - u_H)\|_0 + \|p - p_H\|_0\right) + c_2\alpha_H\|\nabla(u - u_H)\|_0$$
$$+ c_3\|\nabla(u - u_H)\|_0^2 + c_4\alpha_H H\|u\|_2. \tag{23}$$

By applying (10)*, we have with $1 \leq s \leq k$ that*

$$\|\nabla(u - u_H)\|_0 \leq C_1\left(1 + \frac{2}{\sigma}(1 + \kappa_1)\right)H^s + \frac{C_2\alpha_H}{\nu\sigma}, \tag{24}$$

$$\|p - p_H\|_0 \leq C_3\left(1 + \kappa_1 + \frac{2\kappa_1}{\sigma}(1 + \kappa_1)\right)H^s + \frac{C_4(\kappa_1 + \sigma)\alpha_H}{\nu\sigma}, \tag{25}$$

$$\|u - u_H\|_0 + \|p - p_H\|_{-1} \leq C_5\left(1 + \kappa_1 + \frac{2}{\sigma}(1 + \kappa_1)^2\right)H^{s+1} + C_6\left(1 + \frac{1 + \kappa_1 + \sigma}{\nu\sigma}\right)\alpha_H H$$
$$+ C_7\left(1 + \frac{2}{\sigma}(1 + \kappa_1)\right)\alpha_H H^s + C_8\left(1 + \frac{2}{\sigma}(1 + \kappa_1)\right)^2 H^{2s} + C_9\frac{1 + \nu\sigma}{\nu^2\sigma^2}\alpha_H^2. \tag{26}$$

Remark 3.2 The results (24)–(26) show that for the solution (u_H, p_H) to attain the same asymptotic convergence rate $\mathcal{O}(H^s)$ as the classical finite element Galerkin solution, the stabilization parameter α_H should be chosen as $\alpha_H = \mathcal{O}(H^s)$.

Remark 3.3 In general, the choice of the stabilization parameters α_H and α_h not only depends on the mesh parameters H and h, respectively, but also on the viscosity ν of the physical fluid being simulated. However, it is a nontrivial task to derive the explicit dependence of stabilization parameters on the viscosity. In our analysis, we only give the dependence of the stabilization parameters on the mesh parameters.

We now give error estimates for the approximate solution of Step 2.

Theorem 3.2 *Under the conditions of Theorem* 3.1, *the solution* $(u_h^*, p_h^*) \in X_h \times M_h$ *of Step 2 in Algorithm I satisfies for* $1 \leq s \leq k$

$$\|\nabla u_h^*\|_0 \leq \nu^{-1}\|f\|_{-1}, \tag{27}$$

$$\|\nabla(u - u_h^*)\|_0 \leq c_1 \left(2 + \delta N + (\nu + \alpha_h)^{-1}\right) h^s$$
$$+ 2\delta\alpha_h + (\nu + \alpha_h)^{-1}\left\{c_2 \left(1 + \kappa_1 + \frac{2}{\sigma}(1 + \kappa_1)^2\right) H^{s+1}\right.$$
$$+ c_3 \left(1 + \frac{1 + \kappa_1 + \sigma}{\nu\sigma}\right)\alpha_H H + c_4 \left(1 + \frac{2}{\sigma}(1 + \kappa_1)\right)\alpha_H H^s$$
$$\left. + c_5 \left(1 + \frac{2}{\sigma}(1 + \kappa_1)\right)^2 H^{2s} + c_6 \frac{1 + \nu\sigma}{\nu^2\sigma^2}\alpha_H^2\right\}, \tag{28}$$

$$\|p - p_h^*\|_0 \leq c_7 \left(1 + \kappa_2(2 + \delta N + (\nu + \alpha_h)^{-1})\right) h^s + c_8(2\delta\kappa_2 + \nu^{-1})\alpha_h$$
$$+ \left(1 + \kappa_2(\nu + \alpha_h)^{-1}\right)\left\{c_9 \left(1 + \kappa_1 + \frac{2}{\sigma}(1 + \kappa_1)^2\right) H^{s+1}\right.$$
$$+ c_{10} \left(1 + \frac{1 + \kappa_1 + \sigma}{\nu\sigma}\right)\alpha_H H + c_{11} \left(1 + \frac{2}{\sigma}(1 + \kappa_1)\right)\alpha_H H^s$$
$$\left. + c_{12} \left(1 + \frac{2}{\sigma}(1 + \kappa_1)\right)^2 H^{2s} + c_{13} \frac{1 + \nu\sigma}{\nu^2\sigma^2}\alpha_H^2\right\}. \tag{29}$$

Proof Taking $(v_h, q_h) = (u_h^*, p_h^*)$ in (18), using (3), (16) and the Schwarz inequality, we have

$$\nu\|\nabla u_h^*\|_0^2 + \alpha_h\|(I - \Pi_h)\nabla u_h^*\|_0^2 \leq \|f\|_{-1}\|\nabla u_h^*\|_0,$$

which leads to the required result (27).

Subtracting (18) from (6), we obtain

$$(\nu + \alpha_h)(\nabla e_h^*, \nabla v_h) + b(u_H, e_h^*, v_h) - (\nabla \cdot v_h, \theta_h^*) + (\nabla \cdot e_h^*, q_h)$$
$$= \alpha_h(\nabla u, \nabla v_h) - \alpha_h(\Pi_h \nabla u_h^*, \nabla v_h) + b(u_H - u, u, v_h), \quad \forall(v_h, q_h) \in X_h \times M_h, \tag{30}$$

where $(e_h^*, \theta_h^*) = (u - u_h^*, p - p_h^*)$. We assume $(w_h, \lambda_h) \in V_h \times M_h$ be an approximation of (u, p) and set $e_h^* = \chi - \varphi_h$ with $\chi = u - w_h$, $\varphi_h = u_h^* - w_h$. Since $V_h \subset X_h$, limiting $v_h \in V_h$ and setting $q_h = 0$ in (30), we reach

$$(\nu + \alpha_h)(\nabla\varphi_h, \nabla v_h) + b(u_H, \varphi_h, v_h)$$
$$= (\nu + \alpha_h)(\nabla\chi, \nabla v_h) + b(u_H, \chi, v_h) - (\nabla \cdot v_h, p - \lambda_h)$$
$$- \alpha_h(\nabla u, \nabla v_h) + \alpha_h(\Pi_h \nabla u_h^*, \nabla v_h) + b(u - u_H, u, v_h), \quad \forall v_h \in V_h. \tag{31}$$

Taking $v_h = \varphi_h$ in (31), using (3)–(5), (8), (14) (20) and (27) we infer

$$(\nu + \alpha_h)\|\nabla\varphi_h\|_0 \leq (\nu + \alpha_h + N\|\nabla u_H\|_0)\|\nabla\chi\|_0 + \|p - \lambda_h\|_0$$
$$+ \alpha_h(\|\nabla u\|_0 + \|\Pi_h \nabla u_h^*\|_0) + c\|u\|_2\|u - u_H\|_0$$
$$\leq (\nu + \alpha_h + \nu^{-1}N\|f\|_{-1})\|\nabla\chi\|_0 + \|p - \lambda_h\|_0$$
$$+ 2\nu^{-1}\alpha_h\|f\|_{-1} + c\|u\|_2\|u - u_H\|_0 \tag{32}$$

Taking the infimum over $w_h \in V_h$ and $\lambda_h \in M_h$, applying (8), (11) and the triangle inequality, we obtain

$$\|\nabla(u - u_h^*)\|_0 \leq C(\beta)(2 + \delta N) \inf_{w_h \in X_h} \|\nabla(u - w_h)\|_0 + (\nu + \alpha_h)^{-1} \inf_{\lambda_h \in M_h} \|p - \lambda_h\|_0$$
$$+ 2\delta\alpha_h + c_2(\nu + \alpha_h)^{-1}\|u - u_H\|_0. \tag{33}$$

Inserting (10) (with $\mu = h$) and (26) into the right-hand side of estimator (33), we get

$$\|\nabla(u - u_h^*)\|_0 \leq c_1 \left(2 + \delta N + (\nu + \alpha_h)^{-1}\right) h^s + 2\delta\alpha_h + (\nu + \alpha_h)^{-1} \left\{ c_2 \left(1 + \kappa_1 + \frac{2}{\sigma}(1 + \kappa_1)^2\right) H^{s+1}\right.$$
$$+ c_3 \left(1 + \frac{1 + \kappa_1 + \sigma}{\nu\sigma}\right)\alpha_H H + c_4 \left(1 + \frac{2}{\sigma}(1 + \kappa_1)\right)\alpha_H H^s$$
$$\left. + c_5 \left(1 + \frac{2}{\sigma}(1 + \kappa_1)\right)^2 H^{2s} + c_6 \frac{1 + \nu\sigma}{\nu^2\sigma^2}\alpha_H^2 \right\}.$$

The required result (28) follows.

We now give error estimate for the pressure. Taking $q_h = 0$ in (30), applying (4), (8), (14), (20) and the Schwarz inequality, we have

$$(\nabla \cdot v_h, p_h^* - \lambda_h) = (\nabla \cdot v_h, p - \lambda_h) - (\nu + \alpha_h)(\nabla e_h^*, \nabla v_h) - b(u_H, e_h^*, v_h)$$
$$+ b(u - u_H, u, v_h) + \alpha_h(\nabla u, \nabla v_h) - \alpha_h(\Pi_h \nabla u_h^*, \nabla v_h)$$
$$\leq \left(\|p - \lambda_h\|_0 + (\nu + \alpha_h + \nu^{-1}N\|f\|_{-1})\|\nabla e_h^*\|_0\right)\|\nabla v_h\|_0$$
$$+ \left(c\|u\|_2\|u - u_H\|_0 + 2\alpha_h\nu^{-1}\|f\|_{-1}\right)\|\nabla v_h\|_0.$$

The applications of LBB condition and the triangle inequality lead to

$$\|p - p_h^*\|_0 \leq \left(1 + \frac{1}{\beta}\right)\|p - \lambda_h\|_0 + \frac{1}{\beta}\left(\nu + \alpha_h + \nu^{-1}N\|f\|_{-1}\right)\|\nabla e_h^*\|_0 + \frac{c}{\beta}\|u\|_2\|u - u_H\|_0 + \frac{2\alpha_h}{\nu\beta}\|f\|_{-1}.$$

Taking the infimum over $\lambda_h \in M_h$, applying (10), (26) and (28), we obtain

$$\|p - p_h^*\|_0 \leq \left(1 + \frac{1}{\beta}\right)\inf_{\lambda_h \in M_h}\|p - \lambda_h\|_0 + \frac{\kappa_2}{\beta}\|\nabla(u - u_h^*)\|_0 + \frac{c}{\beta}\|u\|_2\|u - u_H\|_0 + \frac{2\alpha_h}{\nu\beta}\|f\|_{-1}$$
$$\leq c_7 \left(1 + \kappa_2(2 + \delta N + (\nu + \alpha_h)^{-1})\right)h^s + c_8(2\delta\kappa_2 + \nu^{-1})\alpha_h$$
$$+ (1 + \kappa_2(\nu + \alpha_h)^{-1})\left\{ c_9 \left(1 + \kappa_1 + \frac{2}{\sigma}(1 + \kappa_1)^2\right) H^{s+1}\right.$$
$$+ c_{10} \left(1 + \frac{1 + \kappa_1 + \sigma}{\nu\sigma}\right)\alpha_H H + c_{11} \left(1 + \frac{2}{\sigma}(1 + \kappa_1)\right)\alpha_H H^s$$
$$\left. + c_{12} \left(1 + \frac{2}{\sigma}(1 + \kappa_1)\right)^2 H^{2s} + c_{13} \frac{1 + \nu\sigma}{\nu^2\sigma^2}\alpha_H^2 \right\},$$

which leads to (29). □

Remark 3.4 From Theorem 3.2, we see that when $H = \mathcal{O}(h^{s/(s+1)})$, $\alpha_h = \mathcal{O}(h^s)$ and $\alpha_H = \mathcal{O}(H^s)$, the desired asymptotic convergence rate $\mathcal{O}(h^s)$ for the solution (u_h^*, p_h^*) is expectedly obtained.

Remark 3.5 Due to technical difficulty, there are terms $(\nu + \alpha_h)^{-1} h^s$ and $(\nu + \alpha_h)^{-1} H^{s+1}$ in the estimates (28) and (29), making the error estimates not being optimal with respect to the viscosity ν. However, compared with the standard two-level Oseen correction method without stabilizations which has a term $\nu^{-1} h^s$ in the error estimates (see, e.g., [24,64,65]), the stabilizations in our method improve the error factor from ν^{-1} to $(\nu + \alpha_h)^{-1}$. It is worth mentioning that the full Navier–Stokes equations with the established stabilization methods have also usually a term $C(\nu^{-1}) h^s$ in their error estimates; for example, there is a term $\nu^{-2} h^s$ in the the error estimator for the streamline diffusion method (see Theorem 4.3 and Remark 4.2 in [66]).

Theorem 3.3 *Under the conditions of Theorem 3.1, the solution $(u^h, p^h) \in X_h \times M_h$ obtained from Algorithm I satisfies for $1 \le s \le k$*

$$\|\nabla u^h\|_0 \le \nu^{-1} \|f\|_{-1} + 2\nu^{-3} N \|f\|_{-1}^2, \tag{34}$$

$$\|\nabla(u - u^h)\|_0 \le c_1 \left\{ 1 + \kappa_2 (\nu + \alpha_h)^{-1} + \delta N \left(2 + \delta N + (\nu + \alpha_h)^{-1} \right) \right\} h^s$$

$$+ c_2 (\nu + \alpha_h)^{-1} \left\{ (1 + \kappa_1)(1 + \delta N) + \frac{2}{\sigma} (1 + \kappa_1)[1 + \delta N(1 + \kappa_1)] \right\} H^{s+1}$$

$$+ c_3 (\nu + \alpha)^{-1} (1 + \delta N) \left(1 + \frac{1 + \kappa_1 + \sigma}{\nu \sigma} \right) \alpha_H H$$

$$+ 2\delta \left(1 + \nu^{-1} \|f\|_{-1} + \delta N \right) \alpha_h + c_4 (1 + \delta N)(\nu + \alpha)^{-1} \left(\frac{1 + \nu \sigma}{\nu^2 \sigma^2} \right) \alpha_H^2, \tag{35}$$

$$\|p - p^h\|_0 \le c_1 \kappa_2 \left\{ 1 + \kappa_2 (\nu + \alpha_h)^{-1} + \delta N \left(2 + \delta N + (\nu + \alpha_h)^{-1} \right) \right\} h^s$$

$$+ c_2 \kappa_2 (\nu + \alpha_h)^{-1} \left\{ (1 + \kappa_1)(1 + \delta N) + \frac{2}{\sigma} (1 + \kappa_1)[1 + \delta N(1 + \kappa_1)] \right\} H^{s+1}$$

$$+ c_3 \kappa_2 (\nu + \alpha)^{-1} (1 + \delta N) \left(1 + \frac{1 + \kappa_1 + \sigma}{\nu \sigma} \right) \alpha_H H$$

$$+ \left\{ 2\kappa_2 \delta (1 + \nu^{-1} \|f\|_{-1} + \delta N) + 2\nu^{-1} \|f\|_1 (1 + \nu^{-2} \|f\|_{-1}) \right\} \alpha_h$$

$$+ c_4 \kappa_2 (1 + \delta N)(\nu + \alpha)^{-1} \left(\frac{1 + \nu \sigma}{\nu^2 \sigma^2} \right) \alpha_H^2. \tag{36}$$

Proof The proof is similar to that for Theorem 3.2. Taking $(v_h, q_h) = (u^h, p^h)$ in (19), using (3), (4), (16), (20), (27), and the Schwarz inequality, we have

$$\nu \|\nabla u^h\|_0^2 + \alpha_h \|(I - \Pi_h)\nabla u^h\|_0^2 \le \|f\|_{-1} \|\nabla u^h\|_0 + N \|\nabla(u_H - u_h^*)\|_0 \|\nabla u_h^*\|_0 \|\nabla u^h\|_0.$$

The applications of (20), (27) and the triangle inequality yield the required result (34).

By setting $(e^h, \theta^h) = (u - u^h, p - p^h)$ and subtracting (19) from (6), we arrive at

$$(\nu + \alpha_h)(\nabla e^h, \nabla v_h) + b(u_H, e^h, v_h) - (\nabla \cdot v_h, \theta^h) + (\nabla \cdot e^h, q_h)$$

$$= \alpha_h (\nabla u, \nabla v_h) - \alpha_h (\Pi_h \nabla u^h, \nabla v_h) + b(u_H - u, u, v_h)$$

$$+ b(u_h^* - u_H, u_h^*, v_h), \quad \forall (v_h, q_h) \in X_h \times M_h. \tag{37}$$

Letting $(w^h, \lambda^h) \in V_h \times M_h$ be an approximation of (u, p), splitting $e^h = \xi - \varphi^h$ with $\xi = u - w^h$, $\varphi^h = u^h - w^h$ and setting $q_h = 0$ in (37), we obtain for all $v_h \in V_h$ that

$$
\begin{aligned}
(\nu + \alpha_h)&(\nabla \varphi^h, \nabla v_h) + b(u_H, \varphi^h, v_h) \\
&= (\nu + \alpha_h)(\nabla \xi, \nabla v_h) + b(u_H, \xi, v_h) - (\nabla \cdot v_h, p - \lambda^h) - \alpha_h(\nabla u, \nabla v_h) \\
&\quad + \alpha_h\big(\Pi_h \nabla u^h, \nabla v_h\big) - b(u_H - u, u, v_h) - b(u_h^* - u_H, u_h^*, v_h).
\end{aligned}
\tag{38}
$$

Noting that

$$
\begin{aligned}
b(u_h^* - u_H, u_h^*, v_h) &= b(u_h^* - u, u_h^*, v_h) + b(u - u_H, u_h^*, v_h) \\
&= b(u_h^* - u, u_h^* - u, v_h) + b(u_h^* - u, u, v_h) \\
&\quad + b(u - u_H, u_h^* - u, v_h) + b(u - u_H, u, v_h),
\end{aligned}
$$

taking $v_h = \varphi^h$ in (38), and applying (3)–(5) and (14), we infer

$$
\begin{aligned}
(\nu + \alpha_h)\|\nabla \varphi_h\|_0 &\leq (\nu + \alpha_h + N\|\nabla u_H\|_0)\|\nabla \xi\|_0 + \|p - \lambda^h\|_0 \\
&\quad + \alpha_h(\|\nabla u\|_0 + \|\nabla u^h\|_0) + c\|u\|_2\|u - u_H\|_0 \\
&\quad + N\|\nabla(u - u_h^*)\|_0^2 + N\|\nabla u\|_0\|\nabla(u - u_h^*)\|_0 \\
&\quad + N\|\nabla(u - u_h^*)\|_0\|\nabla(u - u_H)\|_0.
\end{aligned}
\tag{39}
$$

Taking the infimum over $w^h \in V_h$ and $\lambda^h \in M_h$, applying (8), (10), (11), Theorems 3.1 and 3.2, the triangle inequality, noting that $0 < \alpha_H, \alpha_h, H, h < 1$, and omitting the higher-order terms, we obtain

$$
\begin{aligned}
\|\nabla(u - u^h)\|_0 &\leq \Big(1 + \kappa_2(\nu + \alpha_h)^{-1})\Big) h^s \\
&\quad + 2\delta(1 + \nu^{-2}\|f\|_1)\alpha_h + c(\nu + \alpha_h)^{-1}\|u - u_H\|_0 \\
&\quad + N(\nu + \alpha_h)^{-1}\|\nabla(u - u_h^*)\|_0^2 + \delta N\|\nabla(u - u_h^*)\|_0 \\
&\quad + N(\nu + \alpha_h)^{-1}\|\nabla(u - u_h^*)\|_0\|\nabla(u - u_H)\|_0, \\
&\leq c_1\Big\{1 + \kappa_2(\nu + \alpha_h)^{-1} + \delta N\Big(2 + \delta N + (\nu + \alpha_h)^{-1}\Big)\Big\}h^s \\
&\quad + c_2(\nu + \alpha_h)^{-1}\Big\{(1 + \kappa_1)(1 + \delta N) + \frac{2}{\sigma}(1 + \kappa_1)[1 + \delta N(1 + \kappa_1)]\Big\}H^{s+1} \\
&\quad + c_3(\nu + \alpha)^{-1}(1 + \delta N)\Big(1 + \frac{1 + \kappa_1 + \sigma}{\nu\sigma}\Big)\alpha_H H \\
&\quad + 2\delta\big(1 + \nu^{-1}\|f\|_{-1} + \delta N\big)\alpha_h + c_4(1 + \delta N)\big(\nu + \alpha\big)^{-1}\Big(\frac{1 + \nu\sigma}{\nu^2\sigma^2}\Big)\alpha_H^2.
\end{aligned}
$$

The reminder of the proof follows exactly the same way as for Theorem 3.2.   □

Remark 3.6 From Theorem 3.3, we see that if we choose

$$
H = \mathcal{O}(h^{\frac{s}{s+1}}), \quad \alpha_h = \mathcal{O}(h^s), \quad \alpha_H = \mathcal{O}(H^s),
\tag{40}
$$

the desired asymptotic convergence rate $\mathcal{O}(h^s)$ is expectedly obtained.

Remark 3.7 Comparing Remark 3.6 to Remark 3.4, we see that there is no improvement in the scaling between the coarse and fine meshes for the solution (u^h, p^h) of Step 3 compared with the solution (u_h^*, p_h^*) of Step 2. A similar result was also obtained by Layton and Tobiska in [40], where a coarse mesh correction step is employed based on a full linearization for the nonlinearity in the Navier–Stokes equations. However, although the scaling between the coarse and fine meshes is not improved, we will see in the followed section that there is a significant improvement in accuracy of the solution (u^h, p^h) of Step 3 compared with that of (u_h^*, p_h^*) of Step 2.

4 Numerical results

We present numerical results for two examples in incompressible flow problems. The main goals of this section are to illustrate the numerical performance of the proposed method and to numerically verify its effectiveness. In all the computations reported herein, uniform meshes and Taylor–Hood elements are used for the finite element discretizations, and the public domain software FreeFem++ [67] is used. In addition, the Oseen iterative method (cf. [68]) is applied to solve the nonlinear coarse mesh system. The stopping criteria for the nonlinear iterations is set as 10^{-6}, and the initial guess is obtained by solving a Stokes problem.

4.1 Assessment by the problem with an analytic solution

In this part, we first investigate the asymptotic errors provided by the proposed algorithm, and then compare our method with other related methods to illustrate its effectiveness. For convenience, we present that the exact solution describing the steady flow of an incompressible viscous Newtonian fluid in a bounded domain $\Omega = [0, 1] \times [0, 1] \subset \mathbb{R}^2$ is given by

$$p = 3x^2 + 3y^2 - 2, \quad u = (u_1, u_2)^T,$$
$$u_1(x, y) = 0.5\varphi(x)\varphi'(y), \quad u_2(x, y) = -0.5\varphi(y)\varphi'(x),$$

with polynomial $\varphi(t) = t^2(t - 1)^2$.

It is worth noting that using Taylor–Hood elements, an optimal convergence rate of $\mathcal{O}(h^2)$ in the natural energy norm can be obtained. According to Remark 3.6, we choose the stabilization parameters as $\alpha_H = 0.1H^2$ and $\alpha_h = 0.1h^2$. We set $h = n^{-3}$ ($n = 2, 3, 4, 5, 6$) with H satisfying $H = h^{2/3}$ and compute the finite element solutions applying Algorithm I. Figure 1 describes the errors of the computed solutions with different values of $\nu = 10^{-t}(t = 0, 1, 2, 3, 4)$, from which we see that the numerical results are in good agreement with the theoretical predictions, where optimal convergence rates are obtained. Table 1 compares the computed solutions by our present method, the standard stabilized two-grid Oseen correction method (denoted by *Std-Oseen*) and the one-level finite element variational multiscale method based on two local Gauss integrations [1] (denoted by *One-VMS*) on the fine mesh with $\nu = 0.0001$, where *it* is the nonlinear iteration's count satisfying the stopping criterion for the nonlinear coarse mesh system and the CPU time is the wall time of the program, which includes the mesh generation time, the computing time, and the error computing time. From Table 1 we see that our present method yields better approximate solutions than the standard stabilized two-grid Oseen correction method. Noting that the standard stabilized two-grid Oseen correction method (cf. [24]) consists of the first two steps of our present method, the extra third step in our method increases the accuracy of the solution by nearly two times when $h = 1/125$ and $1/256$, compared with the standard stabilized two-grid Oseen correction method. On the other hand, our method yields approximate solutions with an accuracy comparable to that from the one-level variational multiscale method applied directly on the fine mesh, with a substantial reduce in computational time.

To further investigate the performance of our present method, we fix the mesh sizes as $H = 1/36, h = 1/256$ and then compare our method to other related methods with various viscosities $\nu = 10^{-n}(n = 1, 2, 3, 4, 5, 6)$. The compared methods include the one (denoted by *T-New*) obtained by replacing the linearized term $b(u_H, u^h, v_h)$ in the left-hand side of (19) with $b(u_h^*, u^h, v_h)$ as mentioned in Remark 3.1, the present three-step method without
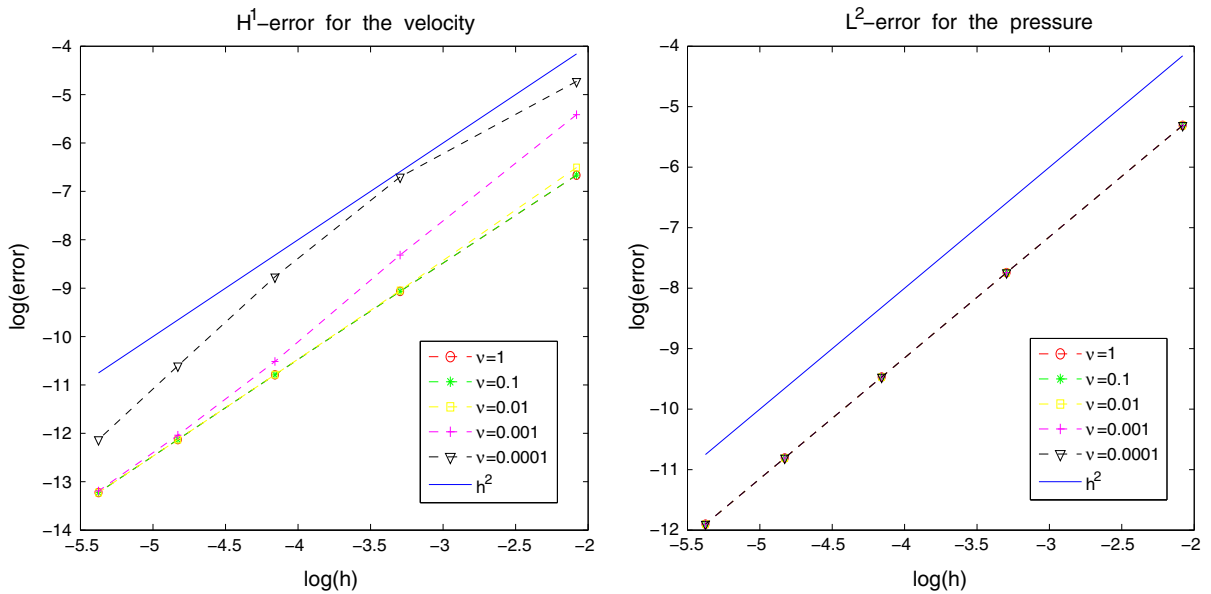
Fig. 1 Errors in H^1-semimorm for the computed velocities (left) and L^2-norm for the pressures (right)

Table 1 A comparison of the computed solutions with $\nu = 0.0001$

Method	h	H	it	CPU(s)	$\|\nabla(u - u^h)\|_0$	$\|p - p^h\|_0$	u_{H^1} rate	p_{L^2} rate
Present	1/8	1/4	5	0.111104	0.00885109	0.00494106	–	–
	1/27	1/9	9	1.17815	0.00122779	0.000433783	1.62392	2
	1/64	1/16	8	5.6903	0.00015578	7.72041×10^{-05}	2.39214	2
	1/125	1/25	8	22.3615	2.47966×10^{-05}	2.02387×10^{-05}	2.74523	1.99999
	1/256	1/36	8	75.3801	5.39433×10^{-06}	6.77866×10^{-06}	2.78877	1.9998
Std-Oseen	1/8	1/4	5	0.079629	0.00945567	0.00494107	–	–
	1/27	1/9	9	0.770729	0.0015577	0.000433784	1.48258	2
	1/64	1/16	8	3.395	0.000241688	7.72042×10^{-05}	2.39214	2
	1/125	1/25	8	12.5667	5.17066×10^{-05}	2.02387×10^{-05}	2.30354	1.99999
	1/256	1/36	8	44.3976	1.42059×10^{-05}	6.77873×10^{-06}	2.36199	1.99978
One-MVS	1/8	–	9	0.313996	0.00874645	0.00494106	–	–
	1/27	–	8	3.34713	0.00122174	0.000433783	1.6182	2
	1/64	–	8	19.6292	0.000153435	7.72041×10^{-05}	2.40399	2
	1/125	–	8	86.3744	2.37394×10^{-05}	2.02387×10^{-05}	2.78765	1.99999
	1/256	–	8	298.152	4.97126×10^{-06}	6.77857×10^{-06}	2.85844	1.99982

stabilizations (i.e., $\alpha_H = \alpha_h = 0$, denoted by *W-Stab*), a four-step Oseen correction method (denoted by *F-Oseen*) obtained by adding an additional fine mesh stabilized Oseen correction step to the present Algorithm I, and a three-step Newton iteration method (denoted by *T-Newton*) which consists of one stabilized coarse mesh nonlinear system and two fine mesh steps of stabilized Newton iterations. Tables 2 and 3 report the computed velocities and the CPU time taken by the methods.

From Table 2 we see that when the viscosity ν is big (not less than 10^{-3}), there is no obvious difference among the computed solutions by the methods being compared. However, when the viscosity is small (less or equal to 10^{-4}), our present method yields solutions with a much higher accuracy than the ones obtained by replacing $b(u_H, u^h, v_h)$

Table 2 A comparison of error $\|\nabla(u - u^h)\|_0$ for the computed solutions u^h by various methods

ν	10^{-1}	10^{-2}	10^{-3}	10^{-4}	10^{-5}	10^{-6}
Present	1.80733×10^{-06}	1.80793×10^{-06}	1.8675×10^{-06}	5.39433×10^{-06}	4.75197×10^{-05}	0.000368516
T-New	1.80733×10^{-06}	1.80801×10^{-06}	1.89131×10^{-06}	1.36087×10^{-05}	0.000308918	0.0020353
W-Stab	1.80732×10^{-06}	1.80732×10^{-06}	1.80732×10^{-06}	1.80789×10^{-06}	1.85887×10^{-06}	–
F-Oseen	1.80733×10^{-06}	1.80793×10^{-06}	1.86747×10^{-06}	4.99212×10^{-06}	4.14871×10^{-05}	0.000226104
T-Newton	1.80733×10^{-06}	1.80793×10^{-06}	1.86747×10^{-06}	4.97125×10^{-06}	4.04561×10^{-05}	0.00019037

Table 3 A comparison of CPU time in second by various methods

| ν	10^{-1}	10^{-2}	10^{-3}	10^{-4}	10^{-5}	10^{-6}
Present	69	69	70	75	77	93
T-New	71	73	72	72	80	95
W-Stab	69	69	80	87	103	–
F-Oseen	106	108	108	110	115	131
T-Newton	80	81	82	85	89	105

**Fig. 2** Lid-driven cavity flow problem
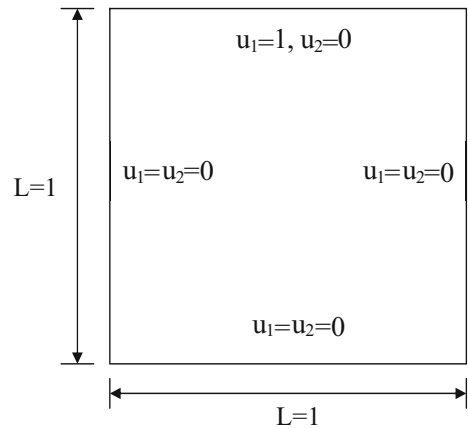
with $b(u_h^*, u^h, v_h)$ in the left-hand side of (19). The method without stabilizations yields better solutions than our present method when $\nu = 10^{-4}$ and 10^{-5}; however, it dosen't work when $\nu = 10^{-6}$ due to the divergence of the iterative method for the nonlinear coarse mesh system, while our present method works well. The numerical results of the four-step Oseen correction method show that further correction doesn't significantly improve the accuracy of the solutions. The accuracy of the computed solutions between our present method and the Newton corrections method is also comparable, except the case $\nu = 10^{-6}$ in which the Newton correction method performs better; however, it takes more CPU time than our present method (see Table 3 for details). We see that from Table 3, when the viscosity is small (i.e., $\nu = 10^{-t}$, $t = 3, 4, 5, 6$), our present method takes the least CPU time among the methods being compared.

4.2 Assessment by the lid-driven cavity flow

We here consider the 2D lid-driven cavity flow. The flow domain is a unit square $[0, 1] \times [0, 1]$ with no-slip boundary conditions, only in the top boundary with $(u_1, u_2)^T = (1, 0)^T$; see Fig. 2 for detailed information.
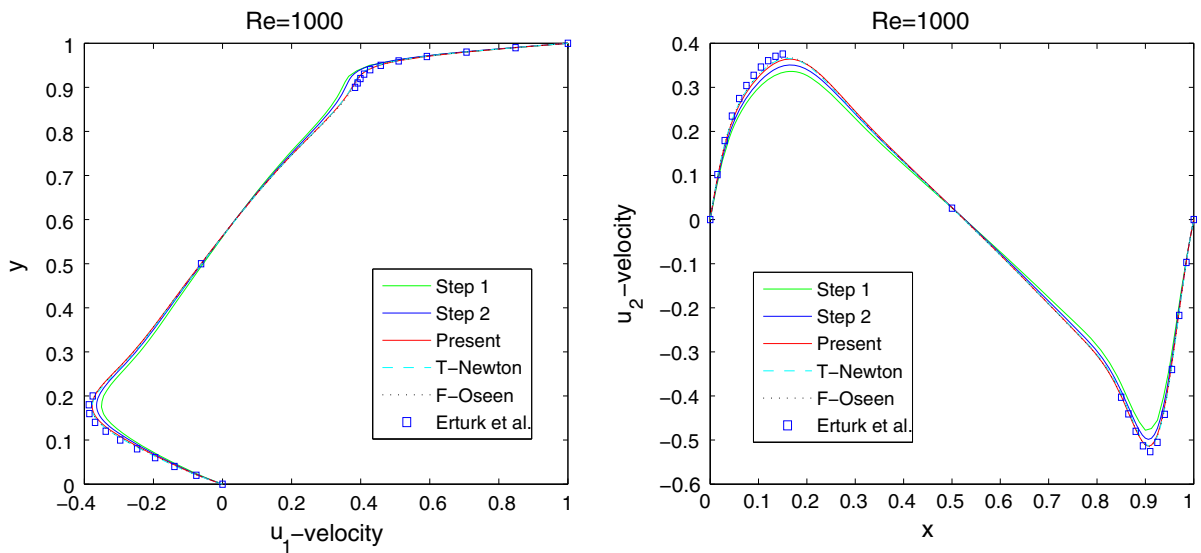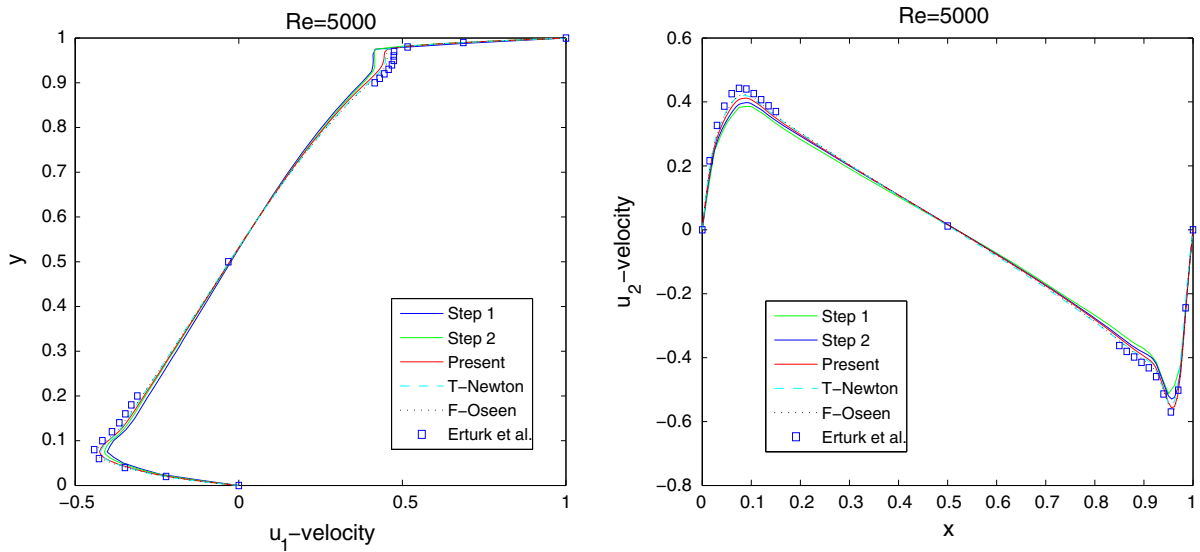
Fig. 3 Comparison of u_1-velocity profiles along the vertical centreline (left) u_2-velocity profiles along the horizontal centreline (right) for the lid-driven cavity flow at $Re = 1000$
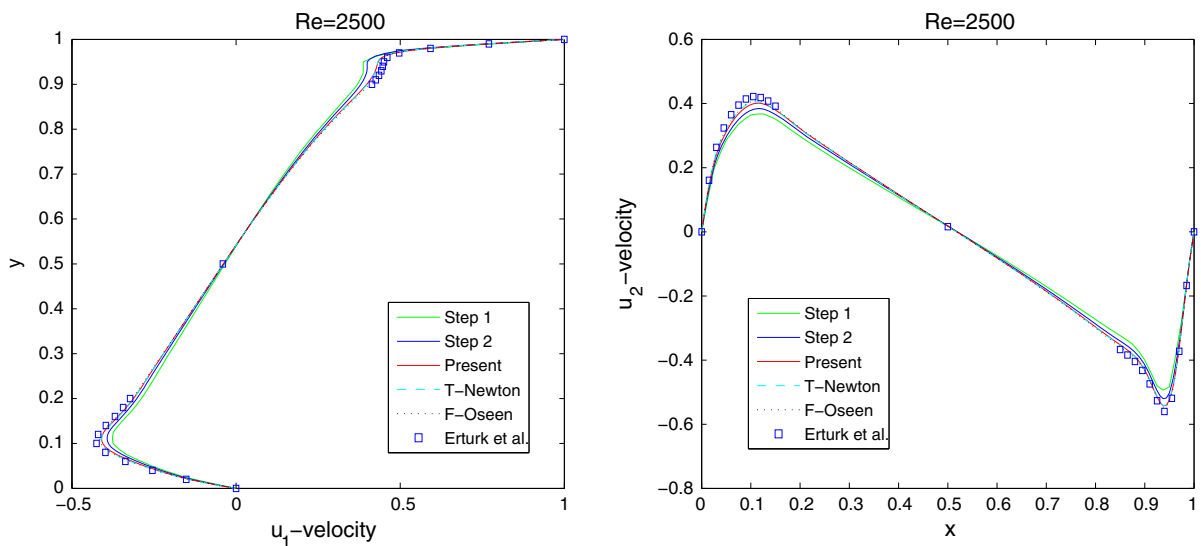
Fig. 4 Comparison of u_1-velocity profiles along the vertical centreline (left) u_2-velocity profiles along the horizontal centreline for the lid-driven cavity flow at $Re = 2500$

In this test case, we set the Reynolds number as $Re = 1000$, 2500 and 5000, where uniform meshes of sizes $H = 1/40$ and $h = 1/160$ are used and the stabilization parameters are set as $\alpha_H = 0.025H$ and $\alpha_h = 0.025h$. We compute the solutions by the first step, the second step and the entire algorithm of present method. For comparison, as done in Sect. 4.1, we also compute the solutions by applying the three-step Newton iteration method (denoted by *T-Newton*) consisted of one stabilized coarse mesh nonlinear system and two steps of stabilized Newton iterations on the fine mesh and the four-step Oseen correction method (denoted by *F-Oseen*) obtained by adding an additional fine mesh third Oseen correction step to the present Algorithm I. Figures 3, 4, 5 compare the numerical results with the existed data of Erturk et al. [69] who used a very fine mesh grid of 601×601. From Figs. 3, 4, 5 we see that each step of our present method significantly improves the accuracy of the approximate solutions of the previous

Fig. 5 Comparison of u_1-velocity profiles along the vertical centreline (left) u_2-velocity profiles along the horizontal centreline for the lid-driven cavity flow at $Re = 5000$

Table 4 CPU time in second spent by the methods for the lid-driven cavity flow

| Re	Step 1	Step 2	Present	T-Newton	F-Oseen
1000 (# 31)	22	38	52	58	68
2500 (# 41)	29	44	59	65	74
5000 (# 60)	42	57	72	78	89

step. Again, noting that the standard stabilized two-grid Oseen correction method consists of the first two steps of our present method, this test case shows that our method can yield an approximate solution with a higher accuracy than the standard stabilized two-grid Oseen correction method. The accuracy of the computed solutions is very comparable among our present method, the three-step Newton iteration method, the four-step Oseen correction method and the data of Erturk et al. [69]. However, our present method spends less CPU time than the three-step Newton iteration method and the four-step Oseen correction method (see Table 4 for details, where the number in bracket is the nonlinear iterations count satisfying the stopping criterion for the nonlinear coarse mesh system). Comparing the numerical results by our present method and that from the four-step Oseen correction method, we see that further iteration does not obviously improve the solutions. Figures 6, 7, 8 describe the computed streamlines and isobars, which are also in good agreement with those in the literature (cf. [69,70]). This test case illustrated the effectiveness of the proposed method.

5 Conclusions

In this work, we proposed and studied a three-step Oseen correction method for the steady incompressible Navier–Stokes equations at high Reynolds numbers. This method uses a two-grid discretization strategy and a finite element variational multiscale approach based on two local Gauss integrations for stabilizations. It is based on a variational multiscale-stabilized small nonlinear coarse mesh system and two Oseen-linearized fine mesh problems which have the same stiffness matrices with only different right-hand sides. The theoretical analysis shows that, with suitable
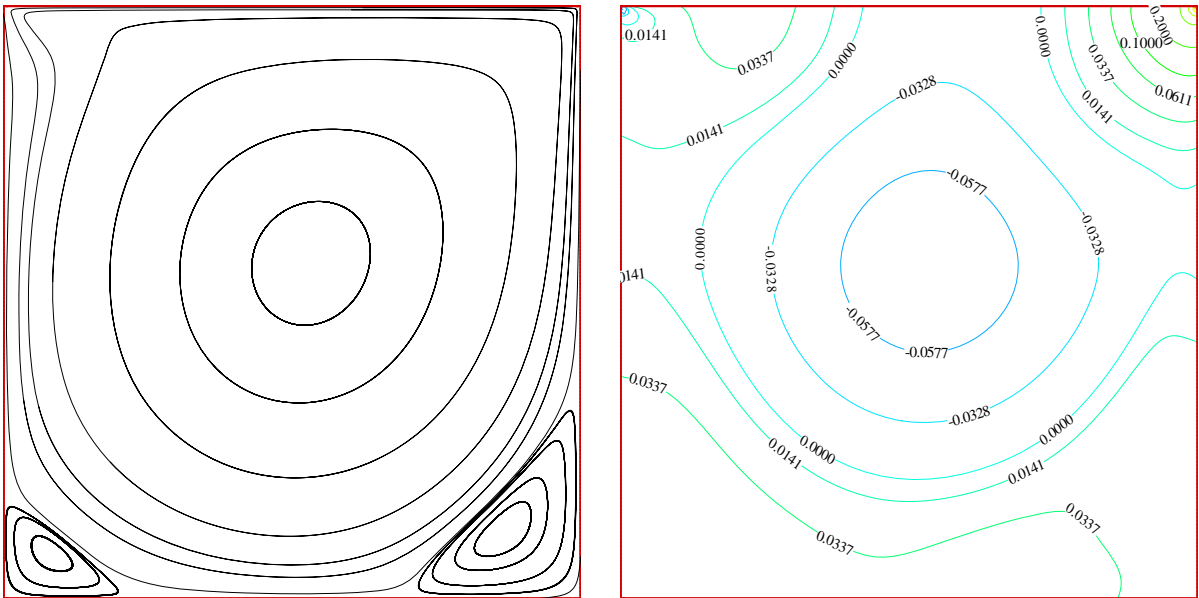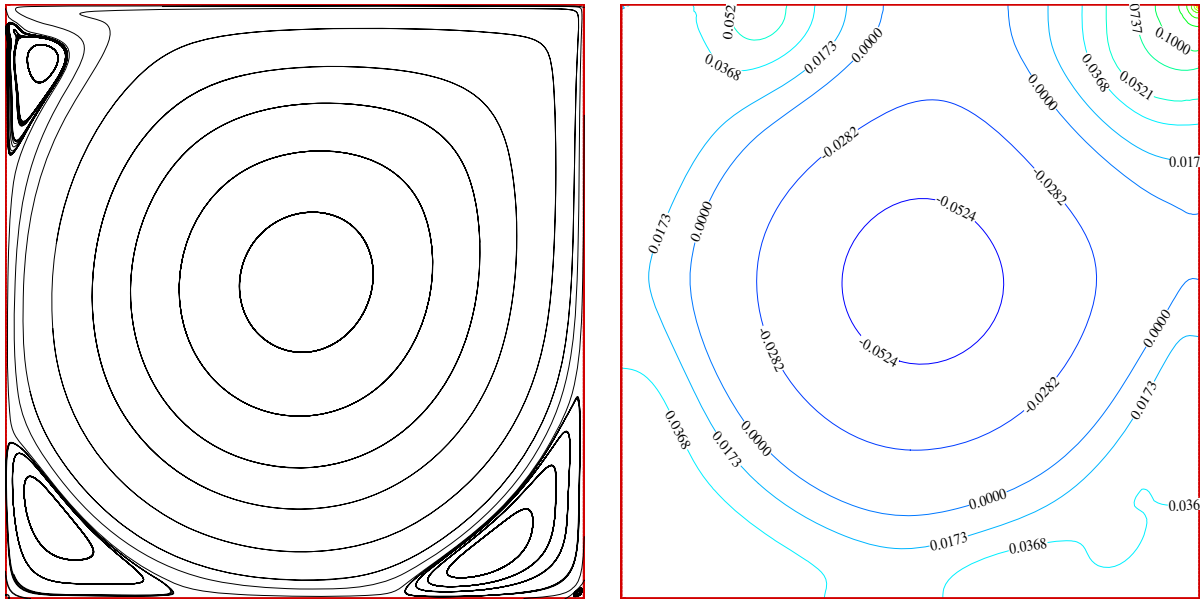
Fig. 6 Computed streamlines (left) and isobars (right) for the lid-driven cavity flow at $Re = 1000$
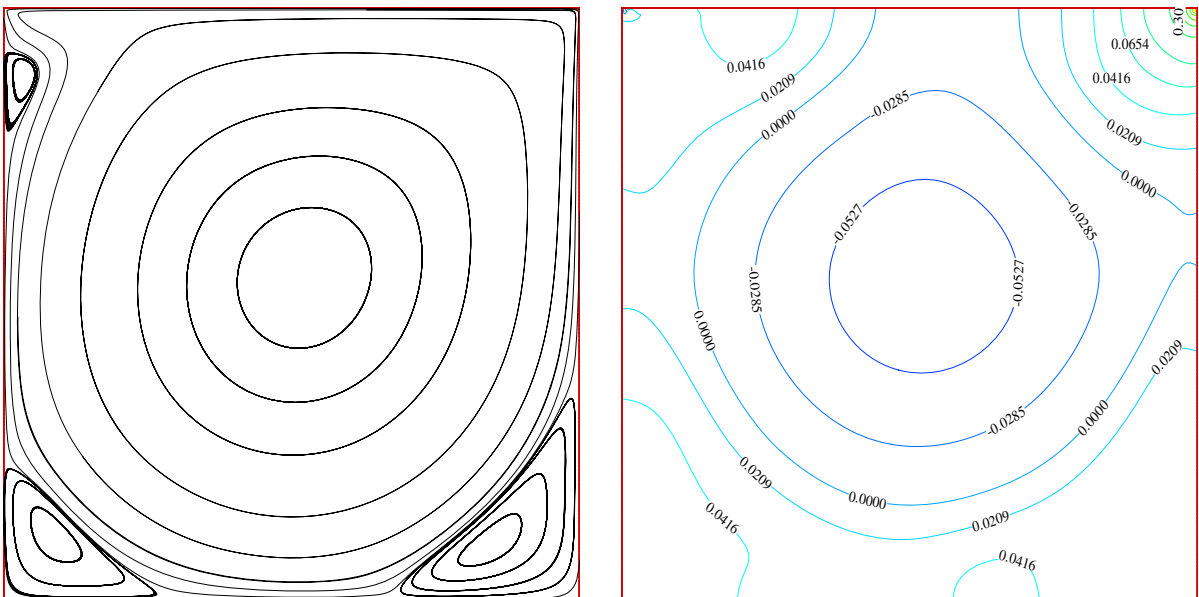
Fig. 7 Computed streamlines (left) and isobars (right) for the lid-driven cavity flow at $Re = 2500$

values of the algorithmic parameters, the proposed method can yield an optimally asymptotic convergence rate. Numerical results demonstrated the effectiveness of the proposed method, which show that the method can yield a convergence rate of the same order as the one-level finite element variational method used directly on the fine mesh, with a substantial reduction in computational time. It can also yield a much better solution with a higher accuracy than the standard stabilized two-grid Oseen correction method.

Fig. 8 Computed streamlines (left) and isobars (right) for the lid-driven cavity flow at $Re = 5000$

References

1. Zheng HB, Hou YR, Shi F, Song LN (2009) A finite element variational multiscale method for incompressible flows based on two local Gauss integrations. J Comput Phys 228:5961–5977
2. Li J, He YN (2008) A stabilized finite element method based on two local Gauss integrations for the Stokes equations. J Comput Appl Math 214:58–65
3. He YN, Li J (2008) A stabilized finite element method based on local polynomial pressure projection for the stationary Navier–Stokes equations. Appl Numer Math 58:1503–1514
4. Bochev P, Dohrmann C, Gunzburger M (2006) Stabilization of low-order mixed finite elements for the Stokes equations. SIAM J Numer Anal 44(1):82–101
5. Roos H-G, Martin Stynes M, Tobiska L (2008) Robust Numerical Methods for Singularly Perturbed Differential Equations – Convection-Diffusion-Reaction and Flow Problems. Springer Series in Computational Mathematics, vol. 24, 2nd ed, Springer, Berlin
6. Arndt D, Dallmann H, Lube G (2015) Local projection FEM stabilization for the time-dependent incompressible Navier–Stokes problem. Numer Methods Partial Differ Equ 31(4):1224–1250
7. Ahmed N, Rebollo TC, John V, Rubino S (2017) A review of variational multiscale methods for the simulation of turbulent incompressible flows. Arch Comput Methods Eng 24:115–164
8. Zheng HB, Hou YR, Shi F (2010) Adaptive finite element variational multiscale method for incompressible flows based on two local Gauss integrations. J Comput Phys 229:7030–7041
9. Shi F, Zheng HB, Yu J, Li Y (2014) On the convergence of variational multiscale methods based on Newton's iteration for the incompressible flows. Appl Math Model 38:5726–5742
10. Xie C, Zheng HB (2014) A parallel variational multiscle method for incompressible flows based on the partition of unity. Int J Numer Anal Model 11(4):854–865
11. Li Y, Mei LQ, Li Y, Zhao K (2013) A two-level variational multiscale method for incompressible flows based on two local Gauss integrations. Numer Methods Partial Differ Equ 29:1986–2003
12. Shang YQ (2013) Error analysis of a fully discrete finite element variational multiscale method for time-dependent incompressible Navier–Stokes equations. Numer Methods Partial Differ Equ 29(6):2025–2046
13. Shang YQ (2013) A parallel two-level finite element variational multiscale method for the Navier–Stokes equations. Nonlinear Anal 84:103–116

14. Shang YQ, Qin J (2017) Parallel finite element variational multiscale algorithms for incompressible flow at high Reynolds numbers. Appl Numer Math 117:1–21

15. Layton W (1993) A two level discretization method for the Navier–Stokes equations. Comput Math Appl 5(26):33–38

16. Shang YQ, Qin J (2016) A finite element variational multiscale method based on two-grid discretization for the steady incompressible Navier–Stokes equations. Comput Methods Appl Mech Engrg 300:182–198

17. Shang YQ, Qin J (2017) A two-parameter stabilized finite element method for incompressible flows. Numer Methods Partial Differ Equ 33:425–444

18. Xu JC (1994) A novel two-grid method for semilinear elliptic equations. SIAM J Sci Comput 15:231–237

19. Xu JC (1996) Two-grid discretization techniques for linear and nonlinear PDEs. SIAM J Numer Anal 33(5):1759–1777

20. He YN, Zhang Y, Xu H (2013) Two-level Newtons method for nonlinear elliptic PDEs. J Sci Comput 57(1):124–45

21. Dai XX, Cheng XL (2008) A two-grid method based on Newton iteration for the Navier–Stokes equations. J Comput Appl Math 220:566–573

22. He YN, Li KT (2005) Two-level stabilized finite element methods for the steady Navier–Stokes problem. Computing 74:337–351

23. He YN, Wang AW (2008) A simplified two-level method for the steady Navier–Stokes equations. Comput Methods Appl Mech Engrg 197:1568–1576

24. He YN, Li J (2011) Two-level methods based on three correction for the 2D/3D steady Navier–Stokes equations. Int J Numer Anal Model Ser B 2(1):42–56

25. He YN, Zhang Y, Shang YQ, Xu H (2012) Two-level Newton iterative method for the 2D/3D steady Navier–Stokes equations. Numer Methods Partial Differ Equ 28(5):1620–1642

26. Liu QF, Hou YR (2010) A two-level finite element method for the Navier–Stokes equations based on a new projection. Appl Math Model 34(2):383–399

27. Shang YQ (2013) A two-level subgrid stabilized Oseen iterative method for the steady Navier–Stokes equations. J Comput Phys 233:210–226

28. Shang YQ, Huang SM (2014) A parallel subgrid stabilized finite element method based on two-grid discretization for simulation of 2D/3D steady incompressible flows. J Sci Comput 60:564–583

29. Shang YQ, He YN, Luo ZD (2011) A comparison of three kinds of local and parallel finite element algorithms based on two-grid discretizations for the stationary Navier–Stokes equations. Comput Fluids 40:249–257

30. Shang YQ (2011) A parallel two-level linearization method for incompressible flow problems. Appl Math Lett 24:364–369

31. Shang YQ, He YN, Kim DW, Zhou XJ (2011) A new parallel finite element algorithm for the stationary Navier–Stokes equations. Finite Elem Anal Des 47:1262–1279

32. Girault V, Lions JL (2001) Two-grid finite element scheme for the transient Navier–Stokes problem. Math Model Numer Anal 35:945–980

33. Olshanskii MA (1999) Two-level method and some a priori estimates in unsteady Navier–Stokes calculations. J Comput Appl Math 104:173–191

34. He YN (2003) Two-level method based on finite element and Crank–Nicolson extrapolation for the time-dependent Navier–Stokes equations. SIAM J Numer Anal 41:1263–1285

35. He YN, Liu KM, Sun WW (2005) Multi-level spectral Galerkin method for the Navier–Stokes equations I: spatial discretization. Numer Math 101:501–522

36. He YN, Liu KM (2005) A multilevel finite element method in space-time for the Navier–Stokes problem. Numer Methods Partial Differ Equ 21:1052–1078

37. He YN, Liu KM (2006) Multi-level spectral Galerkin method for the Navier–Stokes equations II: time discretization. Adv Comput Math 25:403–433

38. Hou YR, Mei LQ (2008) Full discrete two-level correction scheme for Navier–Stokes equations. J Comput Math 26:209–226

39. Abboud H, Girault V, Sayah T (2009) A second order accuracy for a full discretized time-dependent Navier–Stokes equations by a two-grid scheme. Numer Math 114:189–231

40. Layton W, Tobiska L (1998) A two-level method with backtraking for the Navier–Stokes equations. SIAM J Numer Anal 35:2035–2054

41. Shang YQ, He YN (2012) A parallel Oseen-linearized algorithm for the stationary Navier–Stokes equations. Comput Methods Appl Mech Eng 209–212:172–183

42. Huang PZ, Feng XL, He YN (2013) Two-level defect-correction Oseen iterative stabilized finite element methods for the stationary Navier–Stokes equations. Appl Math Model 37:728–741

43. Wang K, Wong YS (2013) Error correction method for Navier–Stokes equations at high Reynolds numbers. J Comput Phys 255:245–265

44. Zhang Y, Xu H, He YN (2015) On two-level Oseen iterative methods for the 2D/3D steady Navier–Stokes equations. Comput Fluids 107:89–99

45. Elman HC, Silvester DJ, Wathen AJ (2005) Finite Elements and Fast Iterative Solvers: With Applications in Incompressible Fluid Dynamics. Oxford University Press, Oxford

46. Elman H, Howle VE, Shadid J et al (2007) Least squares preconditioners for stabilized discretizations of the Navier–Stokes equations. SIAM J Sci Comput 30:290–311

47. Cyr EC, Shadid JN, Tuminaro RS (2012) Stabilization and scalable block preconditioning for the Navier–Stokes equations. J Comput Phys 231:345–363

48. Beaume C (2017) Adaptive stokes preconditioning for steady incompressible flows. Commun Comput Phys 22:494–516
49. Adams R (1975) Sobolev Spaces. Academic Press Inc, New York
50. Temam R (1984) Navier–Stokes Equations: Theory and Numerical Analysis. North-Holland, Amsterdam
51. Girault V, Raviart PA (1986) Finite Element Methods for Navier–Stokes Equations: Theory and Algorithms. Springer, Berlin
52. Heywood JG, Rannacher R (1982) Finite element approximation of the nonstationary Navier–Stokes problem I: regularity of solutions and second-order error estimates for spatial discretization. SIAM J Numer Anal 19(2):275–311
53. He YN, Sun WW (2007) Stability and convergence of the Crank–Nicolson/Adams–Bashforth scheme for the time-dependent Navier–Stokes equations. SIAM J Numer Anal 45:837–869
54. He YN (2008) The Euler implicit/explicit scheme for the 2D time-dependent Navier–Stokes equations with smooth or non-smooth initial data. Math Comput 77:2097–2124
55. Kaya S, Layton W, Rivière B (2006) Subgrid stabilized defect correction methods for the Navier–Stokes equations. SIAM J Numer Anal 44:1639–1654
56. Girault V, Raviart PA (1979) Finite Element Approximation of the Navier–Stokes Equations. Springer, Berlin
57. Hood P, Taylor C (1973) A numerical solution of the Navier–Stokes equations using the finite element technique. Comput Fluids 1:73–100
58. Fortin M (1972) Calcul numérique des ecoulements fluides de Bingham et des fluides Newtoniens incompressible par des méthodes d'eléments finis. Doctoral thesis, Université de Paris VI
59. Crouzeix M, Raviart PA (1973) Conforming and nonconforming finite element methods for solving the stationary Stokes equations. RAIRO Anal Numér 7((R–3)):33–76
60. Mansfield L (1982) Finite element subspaces with optimal rates of convergence for stationary Stokes problem. RAIRO Anal Numér 16:49–66
61. Case M, ErvinV Linke A, Rebholz L (2011) A connection between Scott–Vogelius elements and grad-div stabilized Taylor–Hood FE approximations of the Navier–Stokes equations. SIAM J Numer Anal 49(4):1461–1481
62. Zhang SY (2005) A new family of stable mixed finite elements for the 3D Stokes equations. Math Comp 74:543–554
63. Zhang SY (2011) Quadratic divergence-free finite elements on Powell–Sabin tetrahedral grids. Calcolo 48(3):211–244
64. Layton W, Lenferink W (1995) Two-level Picard and modified Picard methods for the Navier–Stokes equations. Appl Math Comput 69:263–274
65. Zhang Y, Xu H, Yinnian He YN (2015) On two-level Oseen iterative methods for the 2D/3D steady Navier–Stokes equations. Comput Fluids 107:89–99
66. Tobiska L, Verfurth R (1996) Analysis of a streamline diffusion finite element method for the Stokes and Navier–Stokes equations. SIAM J Numer Anal 33(1):107–127
67. Hecht F (2012) New development in FreeFem++. J Numer Math 20(3–4):251–265
68. He YN, Li J (2009) Convergence of three iterative methods based on finite element discretization for the stationary Navier–Stokes equations. Comput Methods Appl Mech Eng 198:1351–1359
69. Erturk E, Corke T, Gökcöl C (2005) Numerical solutions of 2-D steady incompressible driven cavity flow at high Reynolds numbers. Int J Numer Methods Fluids 48:747–774
70. Ghia U, Ghia K, Shin C (1982) High-Re solutions for incompressible flow using the Navier–Stokes equations and a multigrid method. J Comput Phys 48:387–411